Clim Dyn
DOI 10.1007/s00382-016-3144-1

The impact of an extreme case of irrigation on the southeastern United States climate

Christopher Selman[1,2] · **Vasubandhu Misra**[1,2,3]

Received: 9 March 2015 / Accepted: 22 April 2016

Abstract The impacts of irrigation on southeast United States diurnal climate are investigated using simulations from a regional climate model. An extreme case is assumed, wherein irrigation is set to 100 % of field capacity over the growing season of May through October. Irrigation is applied to the root zone layers of 10–40 and 40–100 cm soil layers only. It is found that in this regime there is a pronounced decrease in monthly averaged temperatures in irrigated regions across all months. In non-irrigated areas a slight warming is simulated. Diurnal maximum temperatures in irrigated areas warm, while diurnal minimum temperatures cool. The daytime warming is attributed to an increase in shortwave flux at the surface owing to diminished low cloud cover. Nighttime and daily mean cooling result as a consequence repartitioning of energy into latent heat flux over sensible heat flux, and of a higher net downward ground heat flux. Excess heat is transported into the deep soil layer, preventing a rapidly intensifying positive feedback loop. Both diurnal and monthly average precipitations are reduced over irrigated areas at a magnitude and spatial pattern similar to one another. Due to the excess moisture availability, evaporation is seen to increase, but this is nearly balanced by a corresponding reduction in sensible heat flux. Concomitant with additional moisture availability is an increase in both transient and stationary moisture flux convergences. However, despite the increase, there is a large-scale stabilization of the atmosphere stemming from a cooled surface.

Keywords Regional climate modeling · Irrigation · Diurnal climatology · Diurnal · Southeast United States · Southeast US · Regional model · Agriculture · Anthropogenic influences · Anthropogenic · Climate · Climate change · Regional · Impact · Southeast · Model · Parametrization

1 Introduction

Irrigation has been identified as a significant contributor to regional climatology. For instance, irrigation's impact on precipitation manifests in several ways. Conversion from most non-tropical vegetation types to cropland generally produces increases in precipitation by modifying boundary layer structure and available moisture (Pielke et al. 2007). Transitional regions, between moist and dry areas, have strong soil moisture-precipitation coupling, which can lead to increased rainfall over these regions (Wei and Dirmeyer 2012). Over the Indian subcontinent, irrigation weakens the monsoon heat low, allowing for deeper inland penetration of monsoon circulation and evapotranspiration to produce local precipitation (Saeed et al. 2009). In areas of heavy irrigation, local precipitation is seen to increase, though the precipitation gain is generally less than the loss of water through ET, indicating that irrigation can have a net negative effect on local water budgets (Wei et al. 2013). This increase in ET has a second order effect on atmospheric

Electronic supplementary material The online version of this article (doi:10.1007/s00382-016-3144-1) contains supplementary material, which is available to authorized users.

✉ Christopher Selman
cms05j@my.fsu.edu

[1] Department of Earth, Ocean and Atmospheric Science, Florida State University, Tallahassee, FL, USA

[2] Center for Ocean-Atmospheric Prediction Studies, Florida State University, Tallahassee, FL, USA

[3] Florida Climate Institute, Florida State University, Tallahassee, FL, USA

Published online: 02 May 2016

circulation, strengthening tropical rain belts and modifying the Indian monsoon (Puma and Cook 2012). However, these secondary effects appear to be somewhat model dependent. Similarly, development of strong soil moisture gradients can produce thermally induced, sea breeze-like circulations on land (Ookouchi et al. 1984).

Likewise, land-use change has an observable impact on diurnal variations in temperature (Defries et al. 2002; Oke 1982) and other thermodynamic/hydrologic variables including humidity and evapotranspiration (Sorooshian et al. 2011). Thus, when conducting climatological simulations it is of the utmost importance that land-use is considered, especially in regions like the southeastern United States (SEUS) where diurnal variations are significant (Bastola and Misra 2013). In a related study, Misra et al. (2012) showed that irrigation has an impact on the observed surface temperature trends in the SEUS. In recent years, development of next-generation global and regional climate models has allowed for some capturing of these features with the development of urban extent databases (e.g., Schneider et al. 2009) and regional irrigation maps (e.g., Siebert et al. 2005). However, global climate models continue to use resolutions that are not suited for resolving small-scale, dynamic phenomena (Selman et al. 2013). Hence there remains a need for high-resolution regional climate models. Such models have well-documented skill in resolving both features arising from land-use change and small-scale dynamic phenomena (Kanamaru and Kanamitsu 2008; Misra et al. 2012; Dinapoli and Misra 2012).

The effects of irrigation on diurnal variations of all atmospheric and sub-surface variables are well documented in regions outside of the SEUS. The most noted change is a reduction of globally averaged daytime maximum temperatures (on the order of 0.5–1 K) owing to increased cloud cover (Sacks et al. 2009). It has been noted that this cooling of temperature can potentially mask warming associated with climate change (Lobell et al. 2008). In the Great Plains, application of irrigation in a regional climate model (RCM) caused a cooling in maximum temperatures owing to an increase in latent heat (LHF) and decrease in sensible heat (SHF) (Qian et al. 2013). In addition to this cooling, there exists also a slight warming of nighttime minimum temperatures arising from increased thermal conductivity of the darker, wetter soil (Kanamaru and Kanamitsu 2008). These and other results exhibit some regional and model configuration dependencies (Sorooshian et al. 2012; Lobell et al. 2009). Cooling is generally felt less in regions that are climatologically wet or have an already high soil moisture level (Lobell et al. 2008, 2009). Irrigation implementations that fix the soil moisture values at a specific percentage tend to overestimate evapotranspiration when compared with implementations that add water only when falling below a certain water depletion threshold (Sorooshian et al. 2012).

Changes to the surface energy budget are not observed at just the surface, however. Increases in LH at the surface from irrigation mirrored increases in the mixing ratio of water vapor in the lower atmosphere (Kueppers and Snyder 2012). By extension it is then plausible to assume that addition of irrigation can affect the vertical structure of the atmosphere and boundary layer. Kueppers and Snyder (2012) noted a lowering of the PBL height, which manifested more prominently in a dry year over an irrigated area. Likewise, in the California Central Valley, humidity over irrigated areas was seen to increase by 9–20 % and PBL heights were found to be low as well (Sorooshian et al. 2011). In both studies it was noted that the effects of irrigation did not extend far beyond the irrigated cells.

In the SEUS, diurnal variation of precipitation represents up to nearly 40 % of seasonal variation in the summer (Bastola and Misra 2013). In fact, the diurnal variation of rainfall is a considerably strong and persistent feature of SEUS climatology (Dai and Trenberth et al. 2004). Carbone and Tuttle (2008) claim that the diurnal variability is stronger over the SEUS than in any other region of the contiguous United States. By virtue of these facts, especially when the climatological features of diurnal variations of precipitation are relatively stationary (Dai et al. 2004), it comes as no surprise that the SEUS is climatologically the wettest region of the United States (Chan and Misra 2010). There is however evidence that climate change presents itself in diurnal signals of surface temperature, such as the observed warming in daily minimum temperatures (Zhou et al. 2008; Misra et al. 2012; Misra and Michael 2012). Similarly, that larger-scale climatological phenomenon affected by climate change, such as the North Atlantic Subtropical High, can impart an influence on the diurnal variability of sea breeze circulations (Li et al. 2011; Misra et al. 2011; Selman et al. 2013).

Presently, atmospheric global circulation models (AGCMs) such as those used in CMIP5 are unable to correctly simulate diurnal variations in precipitation and temperature (Dai et al. 1999; Slingo et al. 2004; Braganza et al. 2004; Lewis and Karoly 2013). These deficiencies stem from an improper consideration of land-surface and cloud cover processes, leading to an underestimated trend in the diurnal temperature range (Lewis and Karoly 2013). Improving the simulation of mean rainfall rates can also lead to an improvement in simulation of diurnal rainfall patterns in increased-resolution simulations (Dirmeyer et al. 2012). It has been indicated in multiple studies that use of high-resolution regional climate models can improve erroneous phase shifts and magnitudes of diurnal patterns (Liang et al. 2004; Chow and Chan 2010). These improvements can be traced to shrewd choice of cumulus

parameterization scheme (Liang et al. 2004; Lee et al. 2007; Wang et al. 2007; Evans and Westra 2012; Harding et al. 2013).

By astutely choosing our cumulus parameterization, we are able to better simulate the drivers of diurnal precipitation variability in the SEUS. Such drivers include sea breezes in coastal regions (Schwartz and Bosart 1979; Biggs and Graves 1962; LeMone 1973). Sea breeze effects are especially pronounced in peninsular Florida, where afternoon convergence of sea breezes produces significant convective activity (Byers and Rodebush 1948; Gibson and Vonder Haar 1990). Near the coastline, diurnal precipitation variation can be attributed to convergence of the mean background wind and sea breeze (Gentry and Moore 1954). Farther away from the coast, where no sea breeze is experienced, the interaction of propagating mesoscale systems from the Central United States with background conditions or topography are primary drivers of diurnal variations in precipitation (Parker and Ahijevych 2007).

Diurnal variations in precipitation lead diurnal variations in ground hydrology. The erratic distribution of local convective systems modifies local soil-moisture/precipitation coupling (Wei and Dirmeyer 2012). Due to a lagged timing difference between diurnal temperature and precipitation maxima, partitioning of surface energy into sensible and latent heat flux is influenced by diurnal variations (Selman and Misra 2015). Evapotranspiration, a significant contributor to the water budget of the SEUS (Sun et al. 2002), has an offset diurnal peak from precipitation (1600 UTC, vs. 2200 UTC) (Liu et al. 2005; Stefanova et al. 2012).

Ground hydrology is in large part dictated by soil and vegetative surface type. One of the most readily apparent ways human action can influence ground hydrology is via the application of irrigation (Pielke et al. 2007). Irrigation is modest in the SEUS; Florida withdrew on average 1000–5000 million gallons of water per day in 2005 (Hutson et al. 2000). This is in contrast to California, which withdrew 15,000–25,000, million gallons per day in 2005 (Hutson et al. 2000). This large difference is explained largely by the differing climates of each state. The California Central Valley, a semi-arid/steppe climate, is the most productive agricultural region in the country (McNally et al. 2004), with a gross value of $16 billion for the year 2004 owing to its irrigation withdrawals and year-round mild climate that extends the growing season substantially. The SEUS, a more humid subtropical climate with a similarly long growing season, has profits of $11 billion between Georgia, Florida, Alabama, Mississippi and South Carolina (USDA ERS). However, unlike California, agriculture in the SEUS is largely rain fed. As the agriculture industry of the SEUS grows so too will the demand for water. Thus, the future of agriculture in the SEUS rests on intelligent water management policies similar to those of California, including the adoption of broader irrigation practices.

2 Model description

For this study, we use the regional spectral model (RSM; Kanamitsu et al. 2010). Our chosen region (excluding boundary points where Lehmann nudging occurs; Lehmann 1993) is depicted in Fig. 1. We use RSM to downscale to hourly climate data at a 10 km resolution using NCEP-R2 (Kanamitsu et al. 2002) reanalysis data as both lateral boundary and initial conditions. Soil moisture is initialized directly from the NCEP-R2 data. Integrations are performed over the period 1989–1999, with 1989 discarded as model spin up. We assume the Kain–Fritsch convection

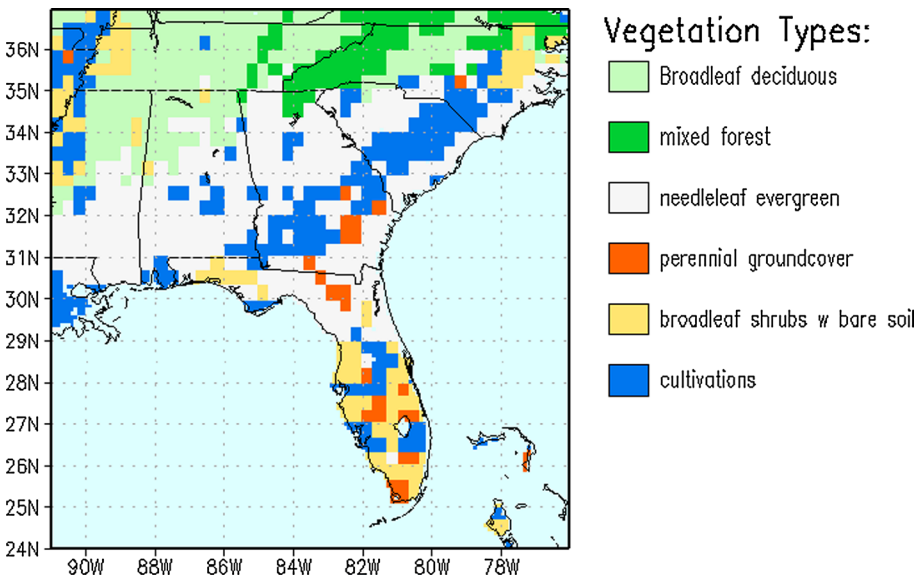

Fig. 1 Domain and vegetation map used in this study

scheme (Kain and Fritsch 1993) In Selman and Misra (2015), it was found that this combination of lateral boundary condition and convection scheme choice produces results with the most reasonable fidelity out of many possible combinations. The RSM in its current configuration is proficient in resolving diurnal variations in the SEUS (Misra et al. 2011; Stefanova et al. 2012; DiNapoli and Misra 2012; Selman et al. 2013). By using a scale selective bias correction technique (Kanamaru and Kanamitsu 2007) we are able to produce simulations that are not sensitive to domain size when downscaling from coarse (2°) resolution data. Importantly, the same scale selective bias correction technique is used for all runs, ensuring that model runs are consistent across comparisons. For the land-surface model, we use the Noah land-surface model (Noah LSM; Ek et al. 2003), using the 12 Noah vegetation types (Loveland et al. 1995) and the 9 soil types of Zobler (1986). Four soil layers, of depths 0–10, 10–40, 40–100 and 100–200 cm are assumed (Mitchell et al. 2005).

Crucial to our study is the modification of the Noah LSM to account for irrigation. The irrigation technique we have chosen to apply to our model is that of a sub-irrigation technique, wherein additional moisture is applied directly to the root zone of the cropland. We choose to use a sub-irrigation technique, as the growing regions of the SEUS have a shallow water table, with table depths in Florida as shallow as 10 cm (Sun et al. 2000). An important feature of sub-irrigation systems is the ability to drain excess water, which we are essentially doing when we constrain the adjusted soil moisture to be not below the wilting point but not above field capacity. Each vegetation type has a specified number of root zones within its parameterization. For the cultivation vegetation type, to which the irrigation is applied, the model has prescribed three root zones, which occupy the span of 0–10, 10–40 and 40–100 cm. Because we employ a sub-irrigation type scheme, we do not moisten the top layer, and instead apply irrigation to the 10–100 cm (root zone) layers. The sub-irrigation process used only by the irrigated runs for this study is summarized in Fig. 2. Note that the control run, which is borrowed from the Selman and Misra (2015) study makes no such considerations, and has not been modified for irrigation whatsoever.

The adjusted LSM in the integrated runs allows the user to specify what fraction of field capacity they would like all irrigated cells to be set at and how long the growing season should be. For the purposes of this study, 100 % of field capacity from the period spanning May to October is chosen. This method carries the weakness that all cells considered to be croplands are fixed to the same percentage of field capacity for the specified months. The real world implication of this is that all municipalities are growing the exact same crop over the same period. Since soil moisture adjustments are being done every time step. This results in

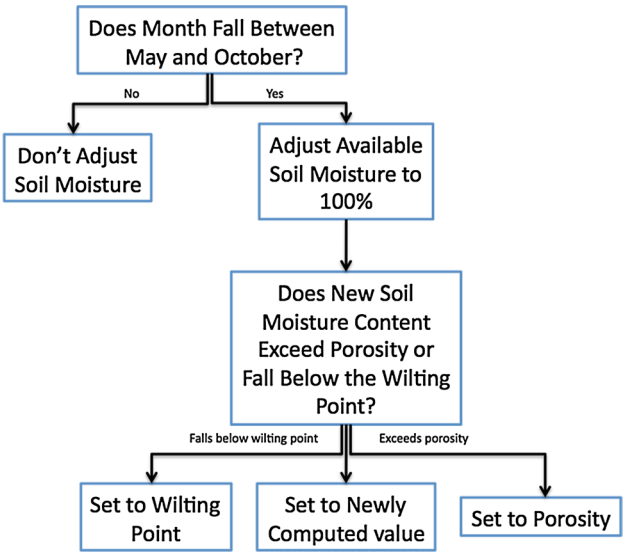

Fig. 2 Flowchart depicting irrigation parameterization within the model

anywhere from 10 to 11 times more water being added to the system than in the real world. This method of irrigation is however similar to some of the previous such studies, which did not keep an account of the water added (Lobell et al. 2006; Kanamaru and Kanamitsu 2008). To understand the implication of this issue on water usage further, we have added a new tracking variable to the model that reports how much water is being added to or taken out of a cell at each time step.

3 Sub-surface irrigation results

3.1 Precipitation

Within the domain, monthly averaged added water during the irrigated period was extreme, often exceeding an average of 200 m of added moisture over the growing season (Fig. 3). However this added water was a consequence of keeping the soil moisture in the root zone at field capacity, which is often the case when growing crops like Rice Paddy. Most water was added to the soil in the month of May (Fig. 3a), which is to be expected, as May is a climatologically drier period than the summer months. As the wet summer season of SEUS was established and diurnal variability of rainfall became prominent, the amount of moisture added reduced over much of the region. Still, it remained incredibly high in magnitude. The amount of water added highlights a critical aspect not previously addressed in similar irrigation studies: Few, if any, studies have indicated the volume of water added to the soil column.

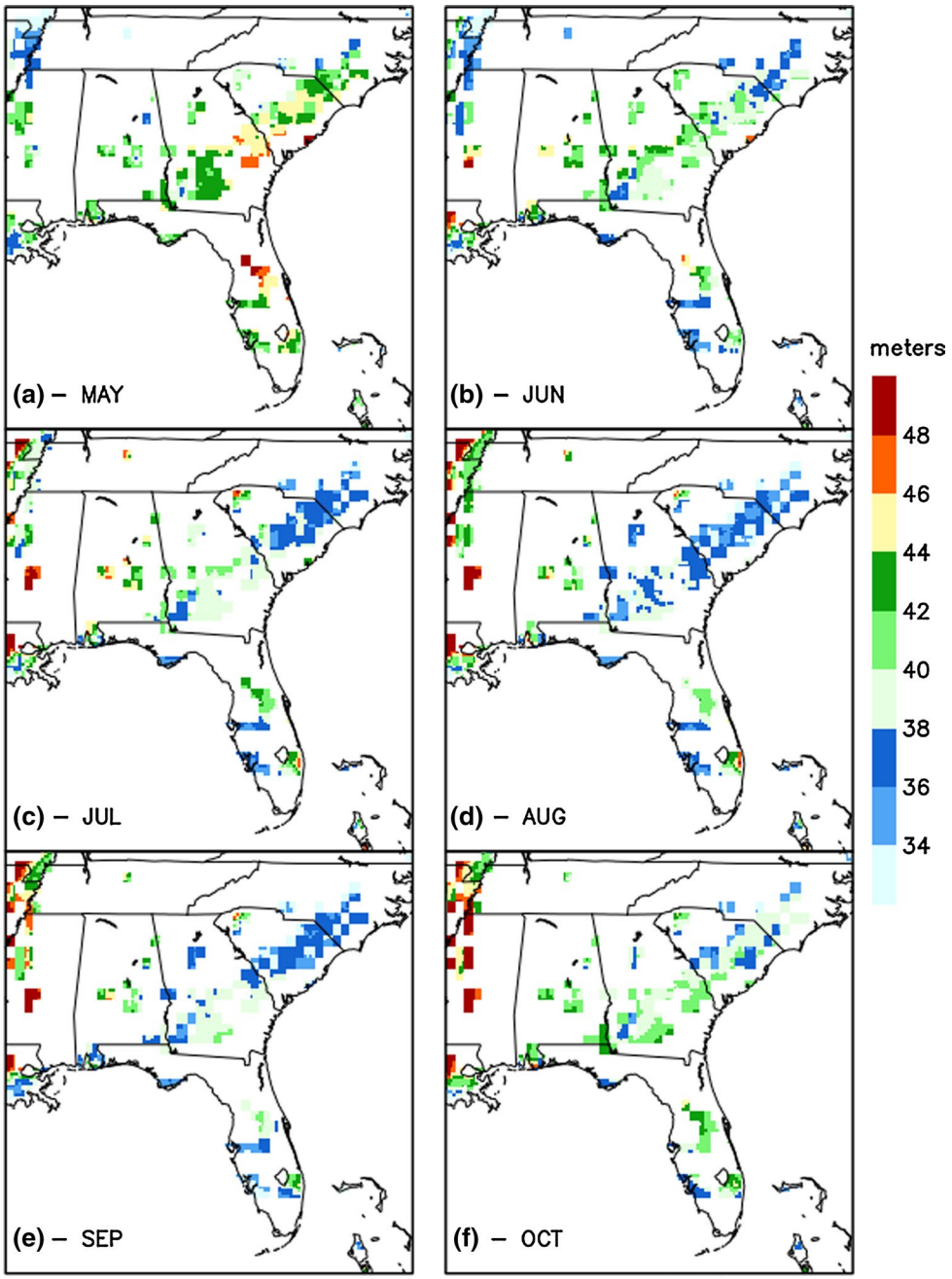

Fig. 3 Monthly average total water added to the soil column

For the monthly climatology, irrigation manifested in precipitation (IRR–CTL) in a mostly local manner, both temporally and spatially (Fig. 4). The impacts of irrigation were most pronounced during the irrigated period (Fig. 4e–j). During this time, there was a pronounced decrease in precipitation above and adjacent to irrigated cells, on the order of 1 mm/day. The sole exception is in June, in which most of the region has an increase in precipitation. There was also an increase in precipitation (again on the order of 1 mm/day) in non-irrigated areas. It is postulated that these patterns are connected via some physical mechanism—likely owing to enhanced atmospheric stability stemming from the altered thermal properties of the moistened surface. These will be discussed in greater detail in Sect. 4. Irrigation impacts on the SEUS climate also appeared to manifest during the non-irrigated season as well (Fig. 4a–d, k, l), though the changes do not seem to follow the same patterns as during the irrigated months. While this study makes no attempt to attribute a physical mechanism to the off-season changes, we hypothesize that the mechanisms could be analogous to other drivers of precipitation change, such as translation speed and intensity of passing cold fronts.

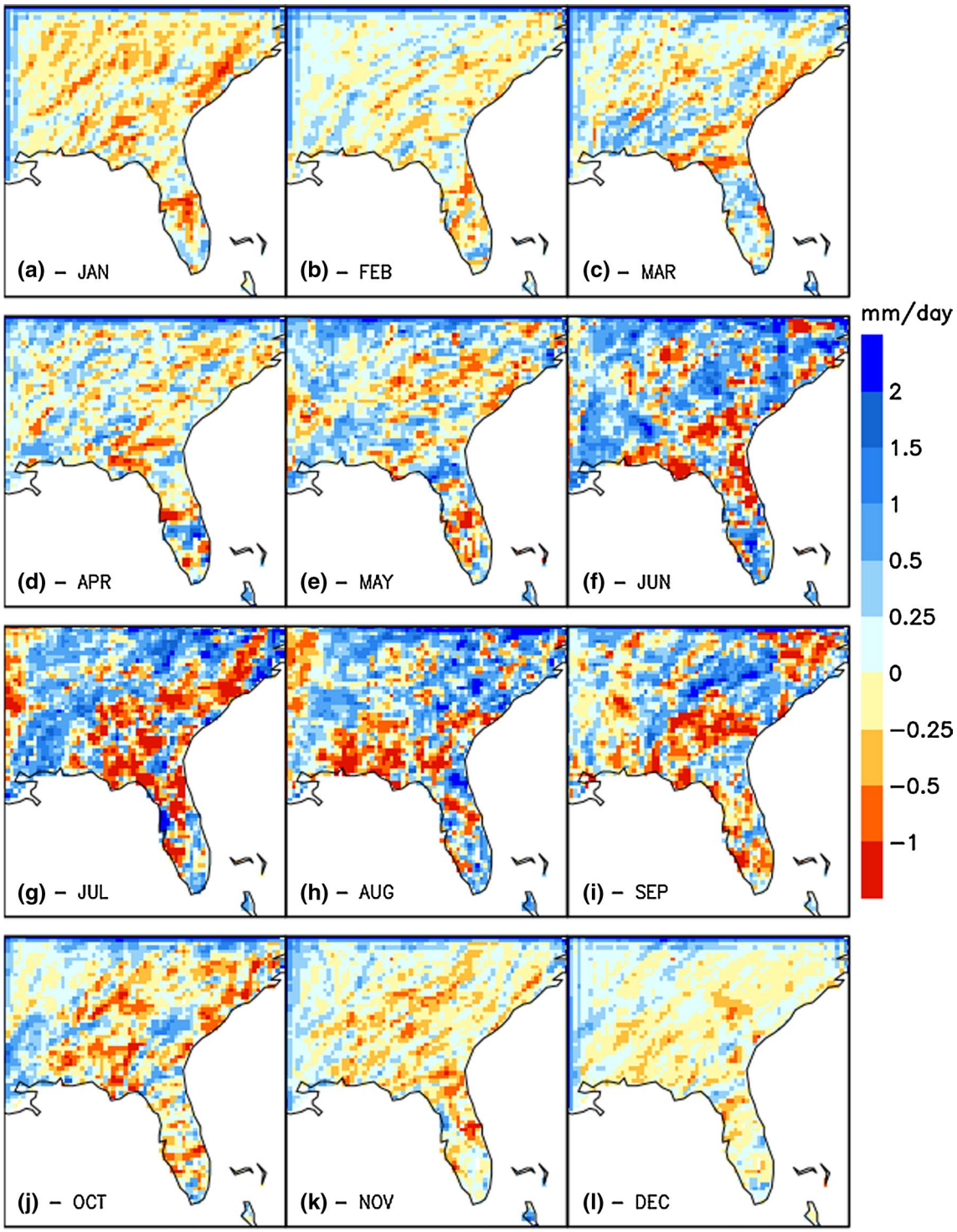

Fig. 4 Monthly average precipitation differences (IRR–CTL)

Changes in diurnal precipitation (IRR–CTL) mirrored those of monthly averaged during the irrigated period (Fig. 5e–j). This was an expected response as diurnal precipitation became stable and pronounced during the irrigated period. Despite changing the amplitude of diurnal precipitation, irrigation did not appear to have an impact on the phase of the diurnal amplitude. This suggests that the changes in precipitation owing to irrigation are not led by one particular mechanism, and instead represent an integrated change (which will be further discussed in Sect. 4). From November to April, the changes in

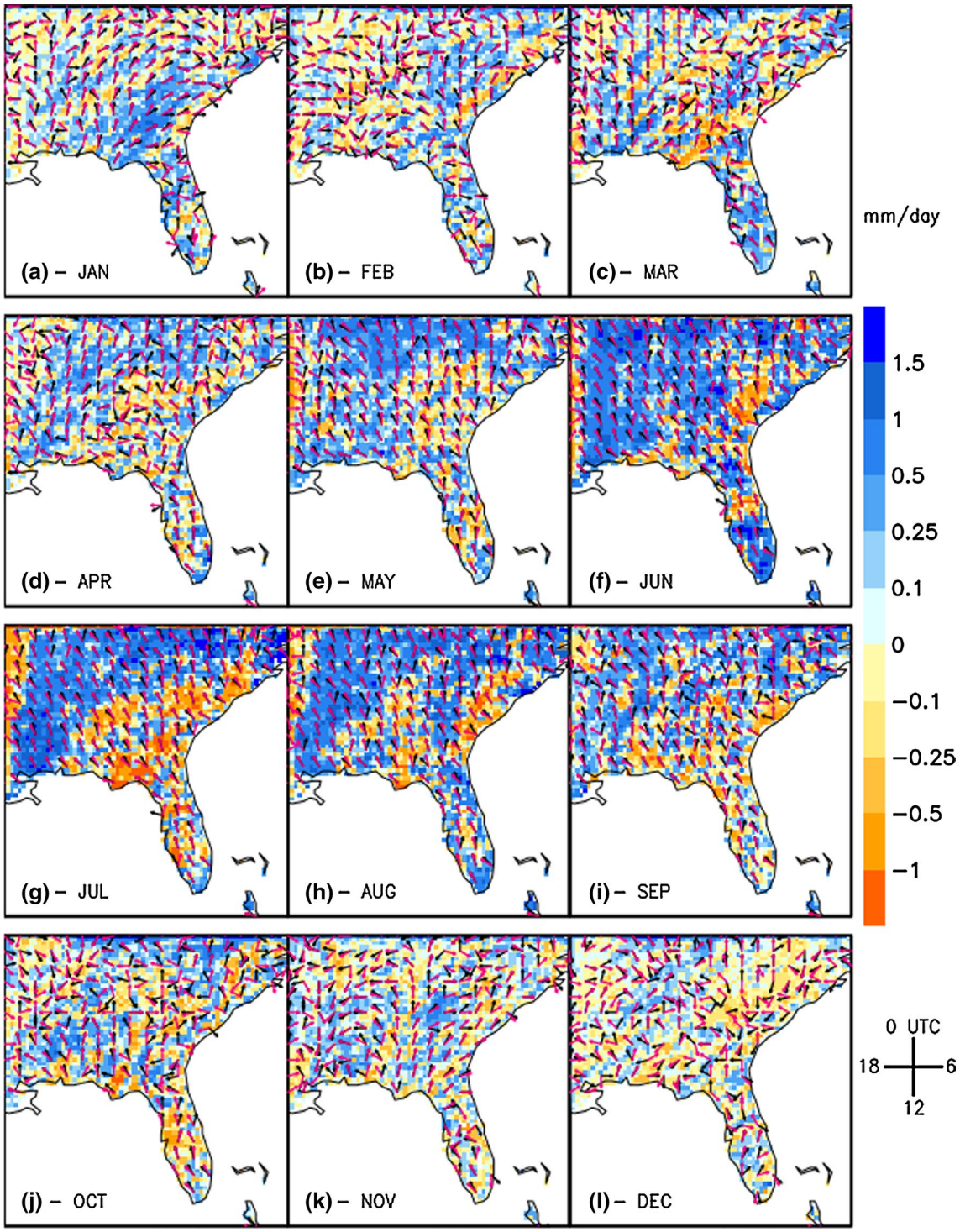

Fig. 5 Diurnal precipitation amplitude differences (IRR–CTL). Overlaid *vectors* indicate the time of maximum rainfall in the IRR simulation (*red*) and CTL simulation (*black*). When only one *vector* is visible, IRR and CTL timing are coincident

diurnal precipitation lack appreciable spatial coherence in both change in amplitude and phase (Fig. 5a–d, k, l). This is owing to relatively weak diurnal variations of precipitation during non-irrigated months in the SEUS.

To understand the nature of precipitation changes caused by irrigation, we binned precipitation events by magnitude (Fig. 6). Bins are separated into 1 mm/day intervals. We confined our binning to areas over irrigated cells only,

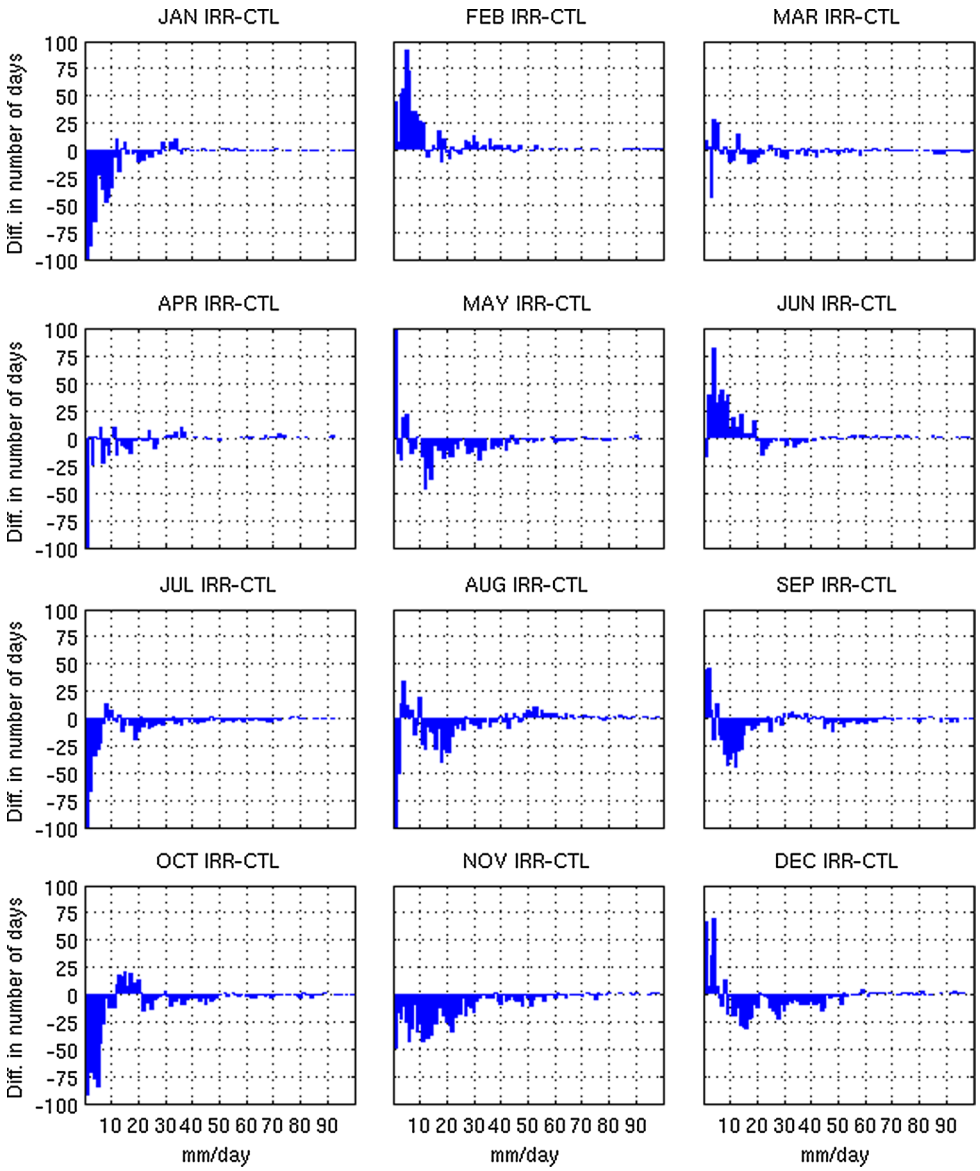

Fig. 6 Binned difference (IRR–CTL) in daily precipitation events. Bins are separated into 1 mm/day intervals

as the impacts of irrigation are primarily seen locally in space. In the irrigated season, with the sole exception of June, there is a decrease in 0–10 and 20 + mm/day events. In each of the irrigated months, there are isolated bins where increases in events are seen, however these are overwhelmed by the net decrease in other rainfall events. Again it is noted that June generally sees an increase in most precipitation events. The response in non-irrigated months is less cohesive; in January, and November there is a net decrease in nearly all precipitation events, yet in February there is a net increase. Thus, these results suggest that there it is a decrease in frequency of small precipitation events (on the order of 1–10 mm/day) that drive the reduction in rainfall during the irrigated season, over irrigated cells.

In order to further understand the reduction in rainfall, we computed moisture budgets over all irrigated cells during the irrigated period (Fig. 7). Terms of the moisture budget are computed as in Selman and Misra (2015). At the onset of the irrigated period, IRR precipitation remains close to CTL, however there is an increase in evaporation and a corresponding decrease in runoff beginning around 1400 UTC. There is also a slight increase in stationary moisture flux convergence. In May, the changes in evaporation and runoff seem to balance each other, causing the IRR residual transient moisture flux convergence (TMFC) to remain close to CTL. From June to August (Fig. 7f–h) the reduction in runoff is greater than the increase in evaporation with an associate increase in TMFC 1600 UTC (smaller negative TMFC in IRR relative to CTL in Fig. 7f–h means there is less transient moisture flux divergence in the former). Therefore despite a net reduction in moisture flux divergence and an increase in surface

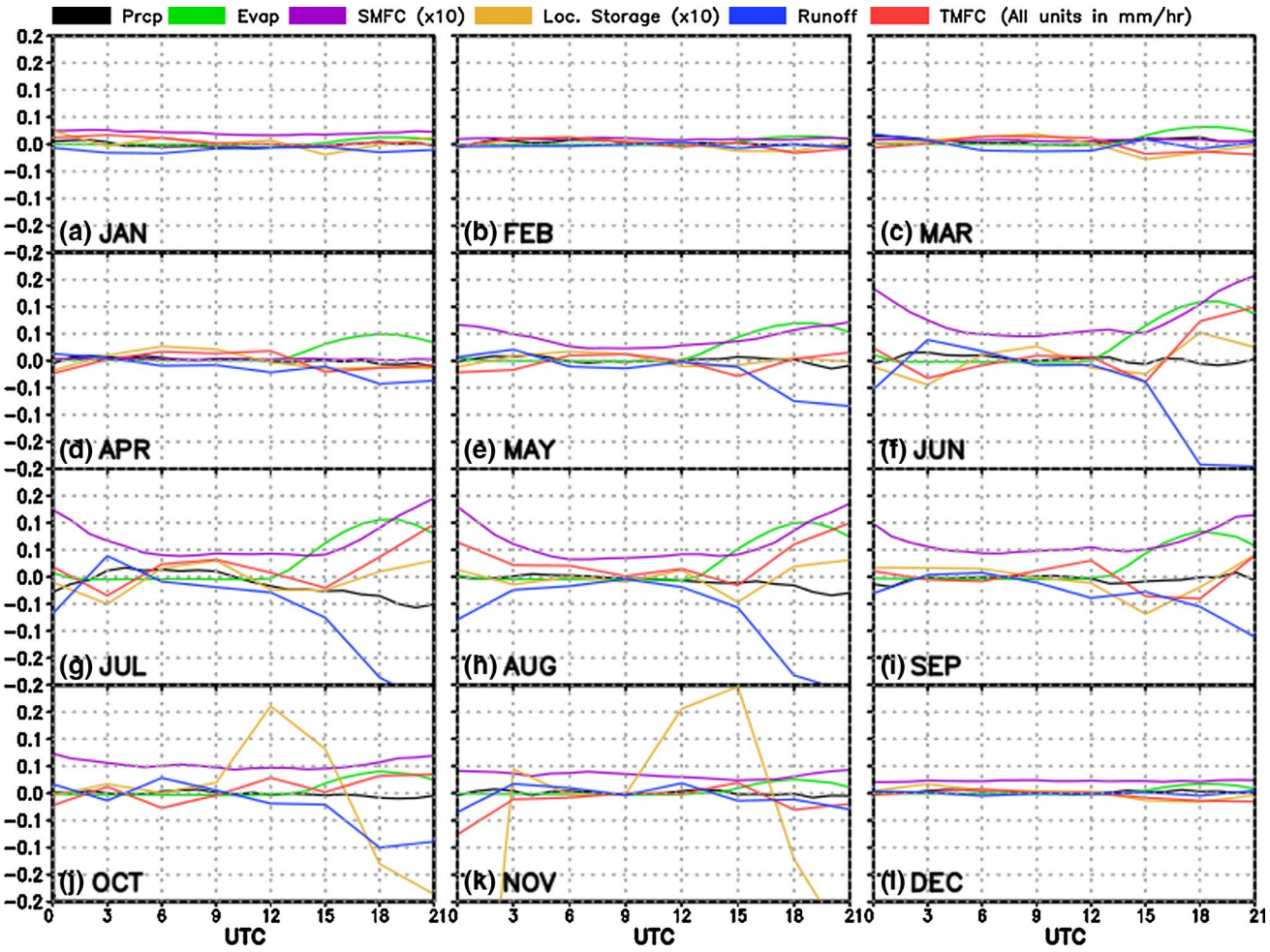

Fig. 7 All terms of the moisture budget for IRR–CTL. For convenience of comparison, both the stationary moisture convergence (SMFC) and local storage are scaled by 10. The transient moisture flux convergence (TMFC) is computed as a residual of all terms

evaporation in the irrigated cells in IRR relative to CTL, there is a net reduction of rainfall in the former relative to the latter, which at the outset is counterintuitive. However we will elaborate further on this reduction in the irrigated cells later in Sect. 4 after discussing the differences in surface temperature.

3.2 Surface temperature

Because irrigation has altered precipitation, and thus by extension cloud cover and radiative and turbulent fluxes, we should expect to see a response in average temperatures. Monthly averaged maximum 2-m temperatures have a noticeable decrease over the irrigated period, with reductions on the order of 0.5 K (Fig. 8). In contrast with precipitation, the effects of irrigation are readily apparent in non-irrigated months, though the decreases in monthly average temperatures are small compared to the changes found in the irrigated months. Outside of the irrigated areas and across all months, it is difficult to make a coherent deduction on change between IRR and CTL (except near the western and northern boundaries of the regional domain; Fig. 8). The notable differences on the western and northern boundaries likely stem from the lateral boundary conditions' lack of consideration for irrigation. Because there are irrigated boundaries in the RSM (Fig. 1) we should expect that some potential discontinuities will exist in the near-boundary relaxation process, and indeed they do manifest in such a way. However, because we believe these areas to be computational, rather than physical, we omit discussion of them and choose to focus primarily on the results farther away from the boundaries. In order to determine the cause of this change in the mean surface temperature between the IRR and CTL integrations, we begin by analyzing the diurnal maximum temperatures (Fig. 9) and the diurnal minimum temperatures (Fig. 10).

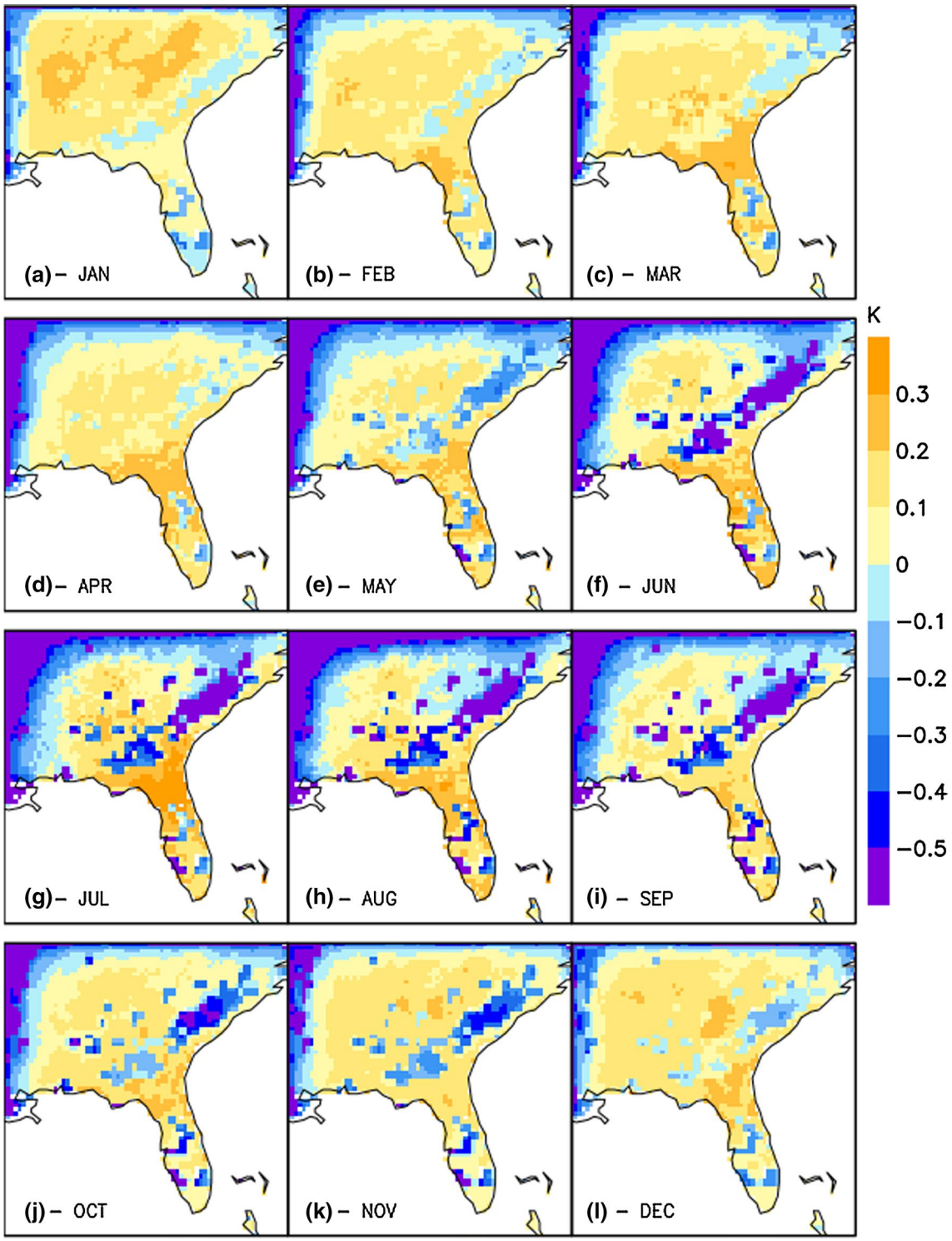

Fig. 8 As in Fig. 4, but for temperature

During the onset of the irrigated period (May), diurnal maximum temperatures change (IRR–CTL) slightly except in Florida, where temperatures rise substantially in IRR relative to CTL (Fig. 9e). In fact, across the entire year, surface temperatures over Florida increase, likely owing to the corresponding reductions in precipitation seen in Fig. 5. By reducing precipitation we have also reduced cloud cover (Fig. 10) and increased insolation. As we will discuss in Sect. 4, into June, many of the irrigated cells in the northeastern portion of the domain cool in IRR compared

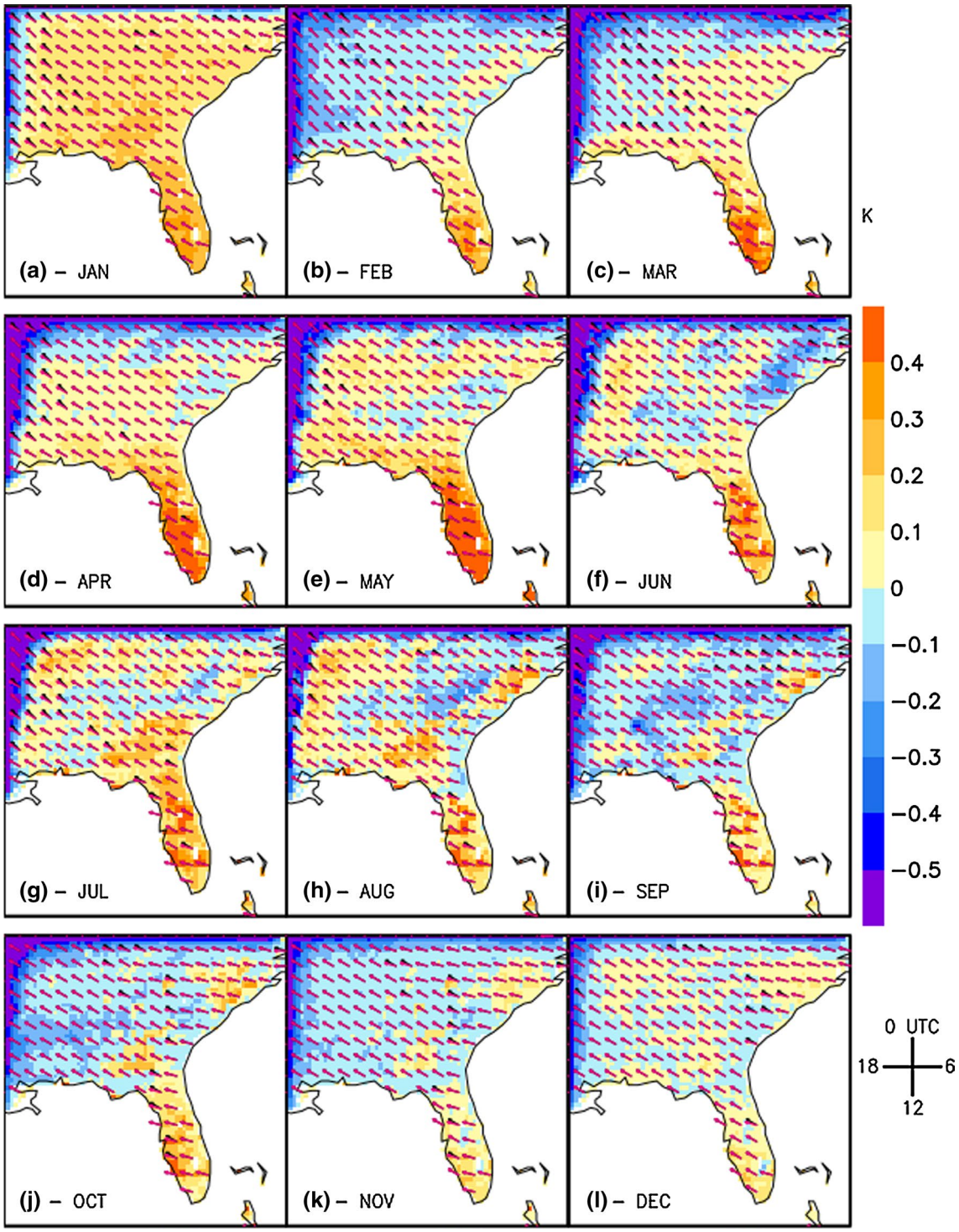

Fig. 9 As in Fig. 5, but for diurnal maximum temperatures

to CTL, despite the corresponding reduction in precipitation (Fig. 9f). However, as the irrigated season progresses, localized warming in diurnal maximum temperature is seen over the irrigated cells, again owing to a reduction in precipitation and cloud cover in IRR relative to CTL. In conjunction with the increase in cloud cover in other non-irrigated areas (Fig. 10), there is an overall reduction in diurnal maximum temperatures over most non-irrigated areas during the irrigated months with the exception in September (Fig. 9i). During non-irrigated months there is

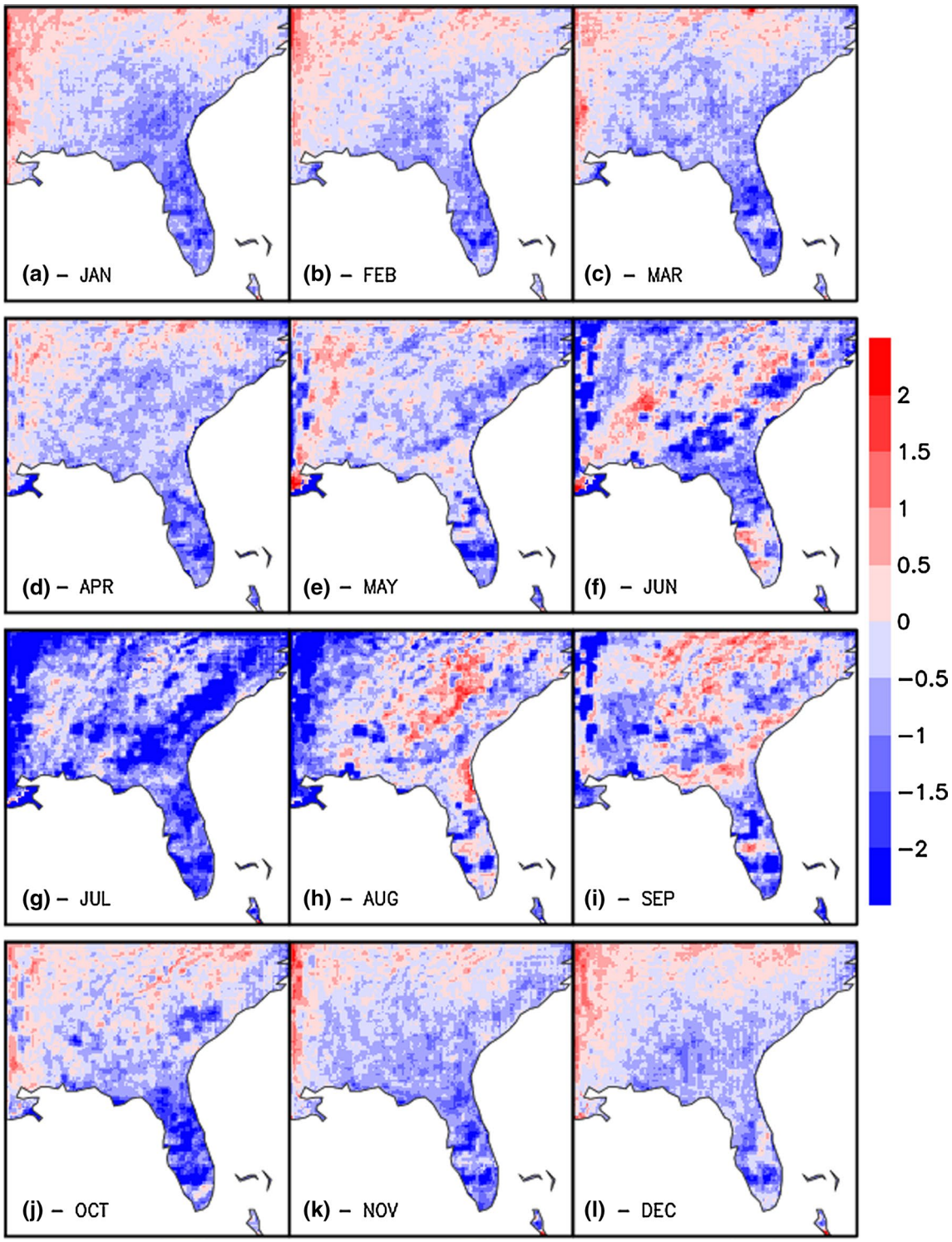

Fig. 10 Difference (IRR–CTL) in low cloud coverage, expressed as a percent of total sky coverage

moderate reduction in diurnal maximum temperature in the IRR run (Fig. 9b, c, j, k, l), owing primarily to overlapping increases in low cloud coverage (Fig. 10b, c, j, k, l). Throughout the year, the phase of the diurnal maximum temperature does not change significantly between IRR and CTL. These patterns of change in diurnal maximum temperatures between the two model integrations are reversed over Florida in analyzing the changes in diurnal minimum

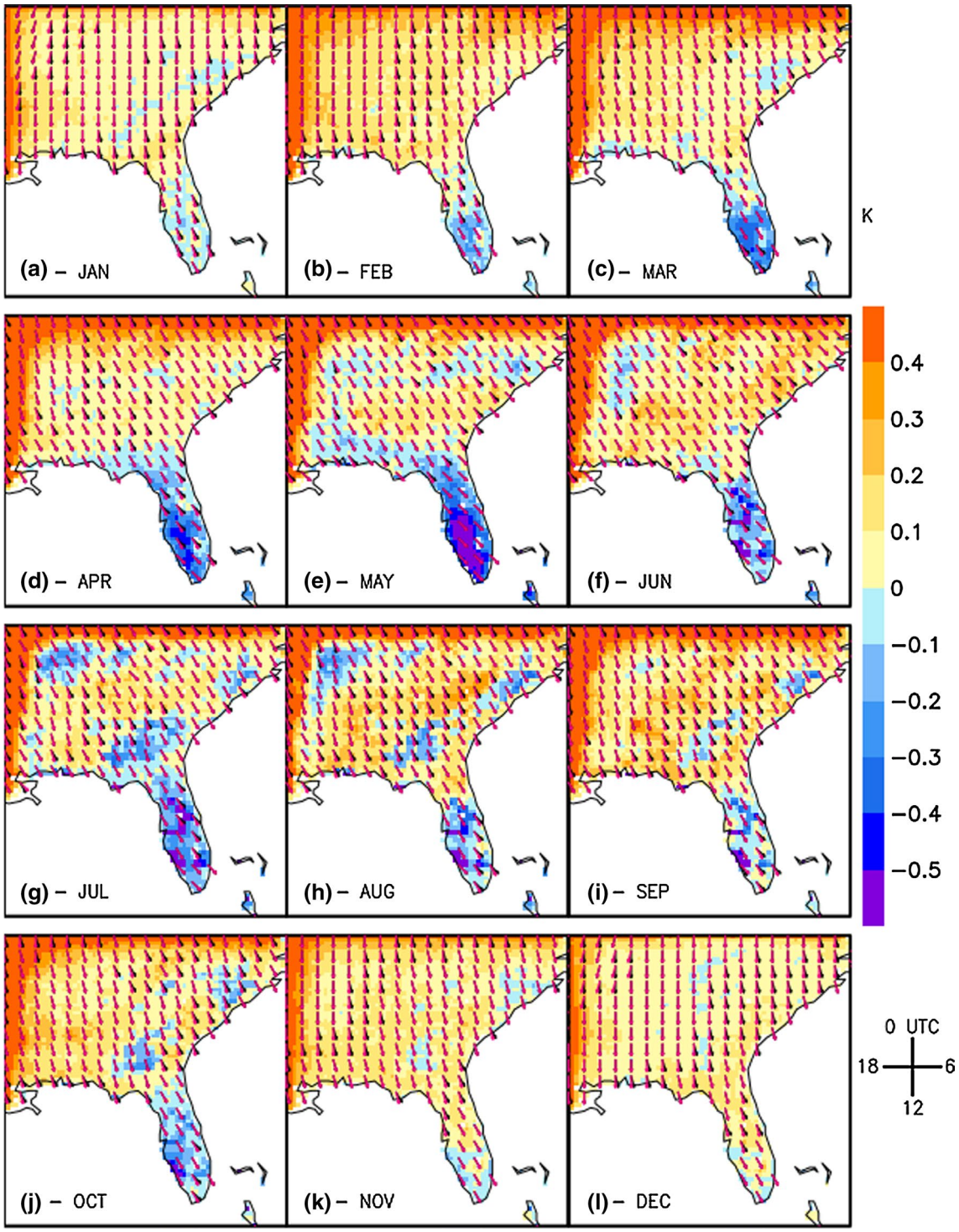

Fig. 11 As in Fig. 9, but for diurnal minimum temperatures

temperatures (Fig. 11). Over irrigated cells, the differences in the diurnal minimum temperature between IRR and CTL is not as systematic, with months of July (Fig. 11g) and August (Fig. 11h) showing some cooling while in May (Fig. 11e) and June (Fig. 11f) showing some warming in IRR integration. Areas of warming and cooling are both present in areas of cloud cover reduction, thus it becomes necessary to break the energy budget down further to understand the mechanisms of change. Interestingly, these analyzed changes do not reconcile the changes in seasonal

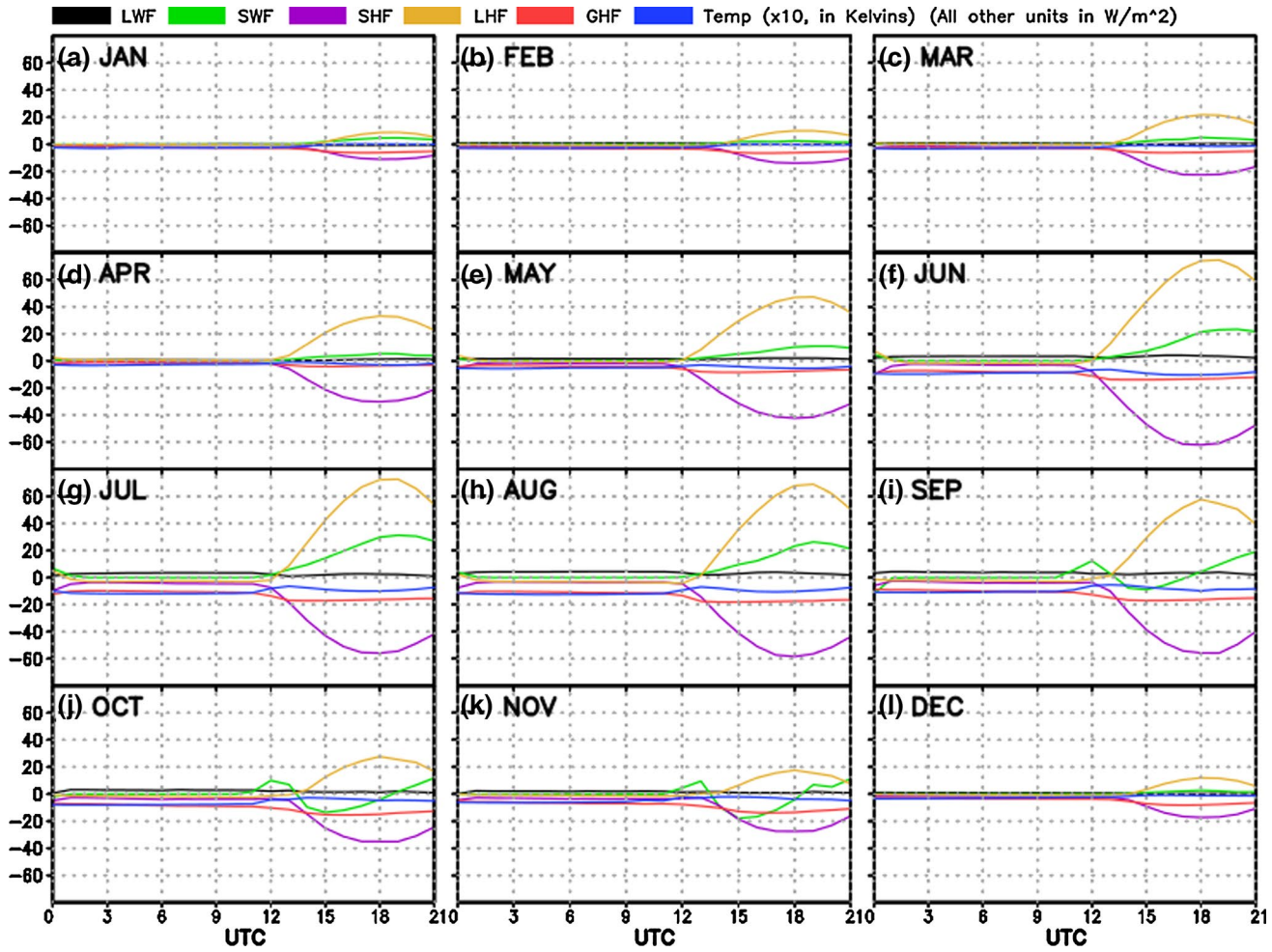

Fig. 12 All terms of the heat budget for IRR–CTL. The signs of each term follow meteorological conventions, with positive values of latent heat flux (LHF), sensible heat flux (SHF) and longwave flux (LWF) indicating upward, and positive values of shortwave flux (SWF) and ground heat flux (GHF) indicating downward. Temperature is also included, but is scaled by ten for visibility purposes

average surface temperatures seen in Fig. 8, which exhibit uniform cooling across all irrigated cells. It is likely, then, that the cooling seen in the monthly averages is driven by changes across other timescales. In fact, analysis of all timescales reveals that no one time scale directly contributes to the cooling seen in the monthly averages, implying that irrigation impacts temperatures across all time scales.

In order that we may understand the mechanisms of temperature change we computed the heat budget (Fig. 12) over all irrigated cells and compared it with the CTL simulation. Throughout the entirety of the irrigated period, the largest changes can be seen in the partitioning of sensible heat flux (SHF) and latent heat flux (LHF). As expected from our above results, LHF increases substantially in IRR (on the order of 60 W/m^2). There is also a moderate increase net shortwave flux during the summer months in the IRR run (Fig. 12f–h), which is to be expected accompanying a reduction in the low cloud cover (Fig. 10). As a consequence of the repartitioning of energy in LHF, there is a corresponding decrease in the SHF in the IRR integration. This repartitioning likely drives the bulk of the cooling in the mean state. However there is a consistent increase in the negative values of the ground heat flux (GHF) in the IRR run. The reduction in GHF can be attributed to the increased sub-surface soil moisture. The addition of water to the subsurface soil (root zone) layers impacts the ground heat flux by introducing a new heat sink at every time step to the surface temperature. Throughout the day, there is a net flux of heat into the sub-surface soil layers (from the top soil to the root zone). During the daytime, this additional downward transport is exceeded by the increase in insolation, driving the daytime warming over the irrigated cells. But at night, with no solar insolation to compensate, the downward heat transport of the GHF adds to the surface temperature cooling induced by the repartitioning of energy into LHF. However, as noted above, some irrigated

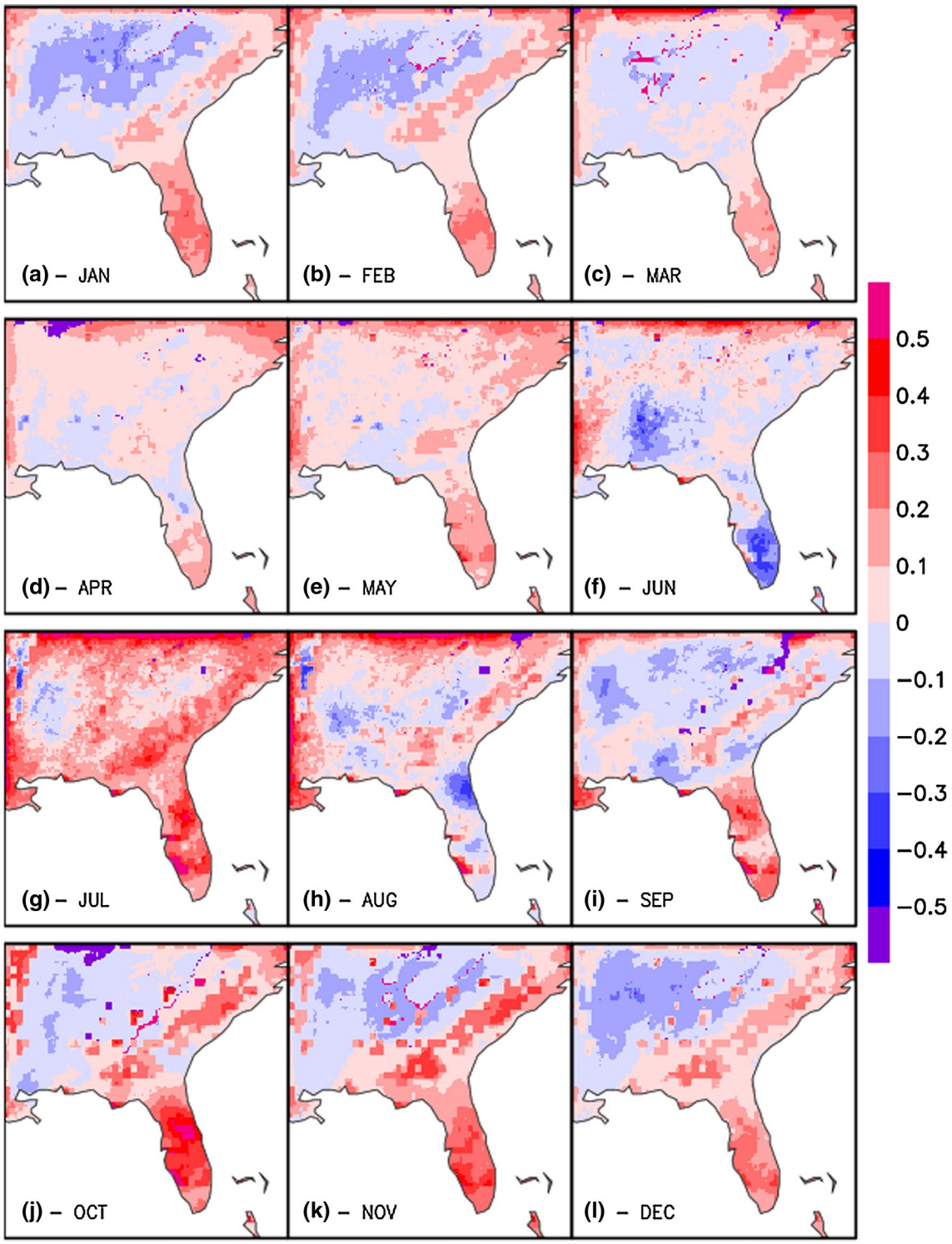

Fig. 13 As in Fig. 8, but for the lifted index (LI). Positive (*negative*) values indicate an atmosphere tending more toward stability (instability)

cells also undergo a nighttime warming, implying that the altered thermal properties of the darker soil may still play a significant role in driving nighttime warming, as in Kanamaru and Kanamitsu (2008).

4 Atmospheric stabilization

In order to identify the causes behind the simulated reduction in precipitation and associated adjustments to the

surface energy budgets, we analyzed atmospheric stability. For this study we chose to analyze the lifted index (LI). LI is computed by lifting a surface parcel dry-adiabatically from the boundary layer to its lifting condensation level, then moist-adiabatically to 500 mb. Negative (Positive) values of LI tend toward atmospheric instability (stability); thus, in the simulated stable atmosphere we should expect higher values of LI in the irrigated run (Fig. 13). Indeed we found that during the irrigated period LI was higher over our irrigated regions (Fig. 13e–h). Notably, in June, there is a substantial decrease in LI over Southern Florida, which in part explains the increase seen in precipitation (Fig. 4f). The increase in LI persists annually, signifying a long-term impact of irrigation in atmospheric stability. However, in months where precipitation variability is primarily driven by transient frontal systems the local stabilization of the atmosphere is overridden by the less-stationary nature of rainfall. In non-irrigated areas there is generally a reduction in the LI, coincident with the simulated increase in precipitation (Fig. 13a–c, f, i–l). A notable exception to this is the month of July, in which there is a near region-wide increase in LI (Fig. 13g). This result appears to be consistent with an overall reduction in low cloud cover (Fig. 10g), though the exact mechanism is not known.

The results presented in this study seem counterintuitive to those performed over other regions, including the California Central Valley. To investigate why these results are unique, we must determine the limiting factor of local hydrology. The SEUS is an energy limited regime, which manifests in relatively smaller influence of irrigation on local precipitation. Since the correlation between precipitation and evaporation over irrigated cells is relatively insignificant (Fig. 14 of supplementary material), it suggests that water added to the soil column will not produce a corresponding increase in precipitation. Addition of irrigation water to soil does not alter this correlation significantly, and as such we only show the correlation for the mean growing season of May–October of the control run. This energy limited regime result is in direct contrast with the California Central Valley, which is a moisture limited regime, owing to the region's arid conditions.

5 Impact of irrigation on simulation validation

Lastly, we turn our attention to how irrigation impacts the validation of our simulations. While it is true that no irrigation of this magnitude occurs in the SEUS, we can still see how our overall root mean square errors (RMSE) of our simulations are impacted by the application of irrigation. We validate our model against the observation data used in Selman and Misra (2015); Temperature data for the period spanning 1990–1999 is taken from the North American Land Data Assimilation System (NLDAS; Cosgrove et al. 2003) and precipitation data from the NCEP stage-IV Radar-derived (stage IV; Lin and Mitchell 2005) rainfall product for the period 2003–2010. The rainfall data is not coincident with our simulation, as stage IV is only available starting in 2002. However, Dai et al. (1999) noted climatological stationarity in the diurnal features of precipitation (e.g., amplitude, phase and spatial patterns) which are unambiguously extracted from both observation and simulation using the Ensemble Empirical Mode Decomposition (EEMD) of Wu et al. (2011).

Figure 16 of supplementary material depicts a monthly time-series of total surface temperature RMSE averaged over all irrigated cells in both CTL and IRR. Application of irrigation to the surface does not appear to have a strong impact in either reducing or increasing the RMSE of surface temperatures over irrigated cells. Ostensibly, this is related to the simulated irrigation's small impact on overall surface temperatures in the SEUS. When the temperature signal is decomposed into its diurnal component, a similar result is found (not shown). We do note, however, that there does seem to be a moderate reduction (on the order of 0.4 K) in RMSE of diurnal temperatures over peninsular Florida as irrigation is applied (not shown.)

Diurnal precipitation RMSE, on the other hand, seems to have a much more pronounced response (Fig. 17 of supplementary material), with an across the board decrease in RMSE. It would appear that the irrigation-induced stabilization of the atmosphere serves to mitigate a positive bias in diurnal precipitation present in our model. This area average is somewhat misleading, however, as the reduction in RMSE is not universally found over the irrigated areas. When we plot a spatial map in the change in RMSE for, say, 2 months with the lowest RMSE in IRR, we find that the RMSE response is heterogeneous in space and time (Fig. 18 of supplementary material).

6 Summary and conclusions

In this study, simulated results of an extreme irrigation case (where irrigation is set to 100 % of field capacity from May through October) were compared against a non-irrigated control run over the SEUS. Studies on this subject in other regions indicated a warming of nighttime temperatures due to increased thermal capacity of moist soil, and cooling of daytime temperatures owing to increased cloud cover. However, over the SEUS our study indicated opposite results-nighttime temperatures cooled and daytime temperatures warmed. These two changes do not explain the staunch cooling tendency seen in the monthly averaged temperatures. It was determined that the pronounced

cooling manifests across all timescales. In order to understand the mechanisms behind these phenomena, surface heat and moisture budgets at hourly interval were computed. It was found that SHF and LHF compensated their respective decreases and increases, and SWF increased at the surface. During the day, the increase in SWF (as a result of less cloud cover) led to an increase in daytime temperatures, and at night an enhanced downward transport in GHF led to nighttime cooling over some irrigated regions. In other regions, the darker soil and reduction in daytime cloud cover caused warming similar to that of Kanamaru and Kanamitsu (2008). The overall decrease in temperature led to a large-scale stabilization of the atmospheric column that persisted through the year, resulting in an overall reduction in cloud cover and by extension precipitation over irrigated areas seen in both the diurnal and monthly averaged values. These changes progress into a positive feedback loop wherein increasing column stability leads to further reduction in rainfall. Because rainfall has reduced, there is a concomitant reduction in cloud cover and increase in downwelling shortwave flux. The increase in shortwave flux then leads to a warming of daytime temperatures. At night, owing to the reduced cloud cover, there is an increased loss of LWF. Alongside this, there is also an increased downward transport of GHF. The two processes combined bring a reduction in nighttime temperatures. The reduction of the cloud fraction in the IRR run is on account of a couple of reasons: (a) the reduction of detrained condensed water from convection and (b) increased stability of the atmosphere in the lower troposphere, which results in the reduction of the diagnosed cloud cover as it fails to meet the threshold stability criterion despite the relative humidity criterion being met. The feedback emerges here, as cooled nighttime temperatures enhance local atmospheric stability. This feedback process is summarized in Fig. 15 of supplementary material. This loop, however, does not become a runaway positive feedback loop. Excess heat from the daytime temperatures is transported downward into the deep soil layers, causing the overall mean cooling of temperatures shown in Fig. 8. The deep soil temperatures take on the bulk of the warming, and because of their heat sink nature, warm slowly over time. In addition to these results, we showed that maintenance of 100 % field capacity irrigation requires an unrealistic amount of water to be maintained through the growing season; on the order of about a 200 m depth of water is added. Previous studies have neglected to consider this, and it is indeed possible over drier regions like the California Central Valley that even more water is being applied than in the SEUS. These results highlight the impact on SEUS climate from an extreme case of sub-surface irrigation.

Despite that, we have found that the mechanisms and features of climatology change owing to irrigation are regionally unique owing to the nature of limiting factor of hydrology; in the case of the California Central Valley, hydrology is moisture limited. We have demonstrated, however, that the Southeast is not moisture limited, but energy limited; the addition of water to the surface in the Southeast will not directly contribute to enhanced precipitation over the region as it would in California. It is possible, too, that sub-regional dependencies exist. For instance, irrigation near topographical features may produce different changes in precipitation than irrigation in a coastal region because of the different drivers of rainfall. If we are to correctly capture anthropogenic influence on climate we must make sure that localized land/atmosphere feedbacks from agriculture are considered. This becomes difficult in GCMs, as different crop specifications must be made over different areas, however it is not outside the realm of possibility that an average crop specification would be usable. Within regional models more rigorous treatment for agriculture should be considered, as temperature or precipitation changes caused by irrigation could mask out or exaggerate broader climate change features. Treatment of irrigation within our model was found to have minimal impact on overall temperature simulation, but a noticeable impact on diurnal precipitation simulation. While this result is somewhat artificial (owing to the exaggerated presentation of irrigation) it still indicates that treatment of irrigation can be crucial in managing biases of simulations.

Importantly, these results have a number of uses for policymakers and stakeholders. The biggest such use would rely on improving the irrigation routines further, such that they could consider actual crop growth and rotation. Pending this, planners could determine optimum schedules for irrigation. Present wisdom indicates that irrigation at night, to reduce water loss from evapotranspiration, is ideal, but if these results are taken as canonical we may see an accelerated cooling of the surface (owing to the partitioning of latent and sensible heat flux and the enhanced ground heat flux) that leads to an even more pronounced stabilization of the atmosphere. Further, optimal spatial distribution of irrigated areas can be derived using different land-surface maps. Spreading irrigation out in smaller, non-adjacent cells could cause a different, less homogenous response in temperature change, and by extension atmospheric stabilization.

In the future, our work will consider more realistic percentages of field capacities on the order of 25–50 %; values that are in line with those of the dominant crops of the SEUS. Because crops are not grown uniformly in time, we are seeking to understand the sensitivity of SEUS climate to varying the vigor of irrigation. We speculate that similar changes found in this study will be present at lower percentages, though their magnitude should be considerably reduced. However, at the lower percentages it is possible

that the dominant mechanisms of change identified in this study may not manifest, and changes that occur could be fundamentally different due to inherent non-linearities.

Acknowledgments This work was supported by Grants from NOAA (NA12OAR4310078, NA10OAR4310215, NA10OAR4320143) and USGS G13AC00408. All model integrations for this paper were done on the computational resourced provided by the Extreme Science and Engineering Discovery Environment (XSEDE) under TG-ATM120010.

References

Bastola S, Misra V (2013) Sensitivity of hydrological simulations of southeastern United States watersheds to temporal aggregation of rainfalls. J Hydrometeorol 14:1334–1344

Biggs W, Graves M (1962) A lake breeze index. J Appl Meteorol Climatol 1:474–480

Braganza K, Karoly D, Arblaster JM (2004) Diurnal temperature range as an index of global climate change during the twentieth century. Geophys Res Lett. doi:10.1029/2004GL019998

Byers H, Rodebush H (1948) Causes of thunderstorms of the Florida peninsula. J Meteorol 5:275–280

Carbone RE, Tuttle JD (2008) Rainfall occurrence in the US warm season: the diurnal cycle. J Clim 21:4132–4146

Chan S, Misra V (2010) A diagnosis of the 1979–2005 extreme rainfall events in the southeastern United States with isentropic moisture tracing. Mon Weather Rev 138:1172–1185

Chow KC, Chan JCL (2010) Diurnal variations of circulation and precipitation in the vicinity of the Tibetan Plateau in early summer. Clim Dyn 32:55–73

Cosgrove B et al (2003) Real-time and retrospective forcing in the North American land data assimilation system (NLDAS) project. J Geophys Res. doi:10.1029/2002JD003118

Dai A, Trenberth KE (2004) The diurnal cycle and its depiction in the community climate system model. J Clim 17:931–951

Dai A, Girgi F, Trenberth KE (1999) Observed and model-simulated diurnal cycles of precipitation over the contiguous United States. J Geophys Res 104:6377–6402

Defries R, Bounoua L, Collatz G (2002) Human modification of the landscape and surface in the next fifty years. Glob Change Biol 8:438–458

Dinapoli S, Misra V (2012) Reconstructing the 20th century high-resolution climate of the southeastern United States. J Geophys Res. doi:10.1029/2012JD018303

Dirmeyer PA et al (2012) Simulating the diurnal cycle of rainfall in global climate models: resolution versus parameterization. Clim Dyn 39:399–418

Ek MB, Mitchell KE, Lin Y, Rogers E, Grunmann P, Koren V, Gayno G, Tarpley JD (2003) Implementation of Noah land surface model advances in the National Centers for Environmental Prediction operational mesoscale Eta model. J Geophys Res 108:8851

Evans JP, Westra S (2012) Investigating the mechanisms of diurnal rainfall variability using a regional climate model. J Clim 25:7232–7247

Gentry R, Moore P (1954) Relation of local and general wind interaction near the seas coast to time and location of air-mass showers. J Atmos Sci 11:507–511

Gibson H, Vonder Haar T (1990) Cloud and convection frequencies over the southeast United States as related to small-scale geographic features. Mon Weather Rev 118:2215–2227

Harding K, Snyder PK, Liess S (2013) Use of dynamical downscaling to improve the simulation of central US warm season precipitation in CMIP5 models. J Geophys Res 118:12522–12536

Hutson S, Barber N, Kenny J, Linsey K, Lumia D, Maupin M (2000) Estimated use of water in the United States in 2000. USGS circular 1268, revised Feb 2005

Kain J, Fritsch M (1993) Convective parameterization for mesoscale models: the Kain-Fritsch Scheme. J Appl Meteorol 43:170–181

Kanamaru H, Kanamitsu M (2007) Scale selective bias correction in a downscaling of global analysis using a regional model. Mon Weather Rev 135:334–350

Kanamaru H, Kanamitsu M (2008) Model diagnosis of nighttime minimum temperature warming during summer due to irrigation in the California Central Valley. J Hydrometall. doi:10.1175/2008JHM967.1

Kanamitsu M, Yoshimura K, Yhang Y, Hong S (2010) Errors of interannual variability and multi-decadal trend in dynamical regional climate downscaling and its corrections. J Geophys Res 115:D17115

Kanamitsu M, Ebisuzaki W, Woollen J, Yang S.-K, Hnilo JJ, Fiorino M, Potter GL (2002) NCEP-DOE AMIP-II Reanalysis (R-2). Bull Amer Meteor Soc 83:1631–1643

Kueppers L, Snyder M (2012) Influence of irrigated agriculture on diurnal surface energy and water fluxes, surface climate and atmospheric circulation in California. Clim Dyn 38:1017–1029

Lee MI et al (2007) Sensitivity to horizontal resolution in the AGCM simulations of warm season diurnal cycle of precipitation over the United States and northern Mexico. J Clim 20:1862–1881

Lehmann R (1993) On the choice of relaxation coefficients for davies lateral boundary scheme for regional weather prediction models. Meteorol Atmos Phys 52:1–14

LeMone MA (1973) The structure and dynamics of horizontal roll vortices in the planetary boundary layer. J Atmos Sci 30:1077–1091

Lewis S, Karoly DJ (2013) Evaluation of historical diurnal temperature range trends in CMIP5 models. J Clim. doi:10.1175/JCLI-D-13-00032.1

Li W, Li L, Fu R, Deng L, Wang H (2011) Changes to the North Atlantic subtropical high and its role in the intensification of summer rainfall variability in the southeastern United States. J Clim 24:1499–1506

Liang X-Z, Li L, Dai A, Kunkel K (2004) Regional climate model simulation of summer precipitation diurnal cycle over the United States. Geophys Res Lett. doi:10.1029/2004GL021054

Lin Y, Mitchell KE (2005) The NCEP stage II/IV hourly precipitation analyses: development and applications. Preprints, 19th conference on hydrology, American Meteorological Society, San Diego, CA, 9–13 Jan 2005, Paper 1.2

Liu S, Graham W, Jacobs J (2005) Daily potential evapotranspiration and diurnal climate forcings: influence on the numerical modeling of soil water dynamics and evapotranspiration. J Hydrol 309:39–52

Lobell D, Bala G, Duffy P (2006) Biogeophysical impacts of cropland management changes on climate. Geophys Res Lett 33:L06708

Lobell D, Bonfils C, Faurès J-M (2008) The role of irrigation expansion in past and future temperature trends. Earth Interact. doi:10.1175/2007EI1241.1

Lobell D, Bala G, Mirin A, Phillips T, Maxwell R, Rotman D (2009) Regional differences in the influence of irrigation on climate. J Clim 22:2248–2255

Loveland TR, Merchant JW, Reed BC, Brown JF, Ohlen DO, Olson P, Hutchinson J (1995) Seasonal land cover regions of the United States. Ann Assoc Am Geogr 85:339–355

McNally A et al (2004) Assessing the region via indicators: the economy. Great Valley Center special report

Misra V, Moeller L, Stefanova L, Chan S, O'Brien JJ, Smith TJ III, Plant N (2011) The influence of atlantic warm pool on panhandle florida sea breeze. J Geophys Res. doi:10.1029/2010JD015367

Misra V, DiNapoli S, Bastola S (2012) Dynamic downscaling of the twentieth-century reanalysis over the southeastern United States. Reg Envrion Change 13:S15–S23

Misra V, Michael J.-P (2012) Varied diagnosis of the observed surface temperature trends in the southeast US. J Clim 26:1467–1472. doi:10.1175/JCLI-D-12-00241.1

Mitchell K et al (2005) User's guide—noah version 2.71. http://www.ral.ucar.edu/research/land/technology/lsm/noah/Noah_LSM_USERGUIDE_2.7.1.pdf

Oke T (1982) The energetic basis of the urban heat island. Q J R Meteorol Soc 108:1–24

Ookouchi Y, Segal M, Kessler RC, Pielke R (1984) Evaluation of soil moisture effects on the generation and modification of mesoscale circulations. Mon Weather Rev 112:2281–2292

Parker MD, Ahijevych DA (2007) Convective episodes in the east-central United States. Mon Weather Rev 135:3707–3727

Pielke RA (1974) A three-dimensional numerical model of the sea breezes over south Florida. Mon Weather Rev 102:115–139

Pielke RA et al (2007) An overview of regional land-use and land-cover impacts on rainfall. Tellus. doi:10.1111/j.1600-0889.2007.00251.x

Puma M, Cook B (2012) Effects of irrigation on global climate during the 20th century. J Geophys Res 115:D16120

Qian Y, Huang M, Yang B, Berg L (2013) A modeling study of irrigation effects on surface fluxes and land–air–cloud interactions in the Southern Great Plains. J Hydrometal 14:700–721

Sacks W, Cook B, Buenning N, Levis S, Helkowski J (2009) Effects of global irrigation on the near-surface climate. Clim Dyn 33:159–175

Saeed F, Hagemann S, Jacob D (2009) Impact of irrigation on the South Asian summer monsoon. Geophys Res Lett 36:L20711

Schneider A, Friedl M, Potere D (2009) A new map of global urban extent from MODIS satellite data. Environ Res Lett 4:044003

Schwartz BE, Bosart LF (1979) The diurnal variability of Florida rainfall. Mon Weather Rev 107:1535–1545

Selman C, Misra V (2015) Simulating diurnal variations over the southeastern United States. J Geophys Res Atmos 120:180–198

Selman C, Misra V, Stefanova L, DiNapoli S, Smith TJ III (2013) Twenty-first-century wet season projections over the southeastern United States. Reg Environ Change. doi:10.1007/s10113-013-0477-8

Siebert S, Döll P, Hoogeveen J, Faures J-M, Frenken K, Feick S (2005) Development and validation of the global map of irrigation areas. Hydrol Earth Syst Sci 9:535–547

Slingo A, Hodges K, Robinson G (2004) Simulation of the diurnal cycle in a climate model and its evaluation using data from Meteosat 7. Q J R Meteorol Soc 130:1449–1467

Sorooshian S, Li J, Hsu K-L, Gao X (2011) How significant is the impact of irrigation on the local hydroclimate in California's Central Valley? Comparison of model results with ground and remote-sensing data. J Geophys Res 116:D06102

Sorooshian S, Li J, Hsu K-L, Gao X (2012) Influence of irrigation schemes used in regional climate models on evapotranspiration estimation: results and comparative studies from California's Central Valley agricultural regions. J Geophys Res 117:D06107

Stefanova L, Misra V, Chan S, O'Brien JJ, Smith TJ III (2012) A proxy for high resolution regional reanalysis for the Southeast United States: assessment of precipitation variability. Clim Dyn. doi:10.1007/s00382-011-1230-y

Sun G, Riekerk H, Kornhak L (2000) Ground-water table rise after forest harvesting on cypress-pine flatwoods in Florida. Wetlands 20:101–112

Sun G, McNulty SG, Amatya DM, Skaggs RW, Swift LW, Shepard JP, Riekerk H (2002) A comparison of the hydrology of the coastal forested wetlands/pine flatwoods and the mountainous uplands in the southern US. J Hydrol 263:92–104

Wang Y, Zhou L, Hamilton K (2007) Effect of convective entrainment/detrainment on simulation of tropical precipitation diurnal cycle. Mon Weather Rev 135:567–585

Wei J, Dirmeyer P (2012) Dissecting soil moisture-precipitation coupling. Geophys Res Lett. doi:10.1029/2012GL053038

Wei J, Dirmeyer P, Wisser D, Bosilovich M, Mocko D (2013) Where does the irrigation water go? an estimate of the contribution of irrigation to precipitation using MERRA. J Hydrometall. doi:10.1175/JHM-D-12-079.1

Wu Z, Huang N, Wallace J, Smoliak B, Chen X (2011) On the time-varying trend in global-mean surface temperature. Clim Dyn 32:429–440

Zhou L, Dai A, Dai Y, Vose RS, Zou C-Z, Tian Y, Chen H (2008) Spatial dependence of diurnal temperature range trends on precipitation from 1950 to 2004. Clim Dyn 32:429–440

Zobler L (1986) A world soil file for global climate modeling. NASA technical memorandum 87802